Synthesis and Cell-Based Activity of a Potent and Selective Protein Tyrosine Phosphatase 1B Inhibitor Prodrug

Irene G. Boutselis,[†] Xiao Yu,[‡] Zhong-Yin Zhang,[‡] and Richard F. Borch*,[†]

Department of Medicinal Chemistry and Molecular Pharmacology and the Cancer Center, Purdue University, West Lafayette, Indiana 47907, Department of Biochemistry and Molecular Biology, Indiana University School of Medicine, Indianapolis, Indiana 46202

Received October 3, 2006

Our laboratory recently reported the development of novel prodrug chemistry for the intracellular delivery of phosphotyrosine mimetics. This chemistry has now been adapted for the synthesis of a prodrug that delivers the nonhydrolyzable difluoromethylphosphonate moiety intracellularly. Activation of the prodrug generates a difluoromethylphosphonamidate anion that undergoes subsequent cyclization and hydrolysis with a $t_{1/2} = 44$ min. A highly potent and selective inhibitor of protein tyrosine phosphatase 1B (PTP1B) with a nanomolar K_i has been reported, but this bis(difluoromethylphosphonate) lacks potential utility due to its exceedingly low membrane permeability at physiological pH. A prodrug of this inhibitor has been synthesized and evaluated in a cell-based assay. The prodrug exhibits nanomolar PTP1B inhibitory activity in this assay, confirming the efficacy of intracellular phosphonate delivery using this prodrug approach.

Introduction

Protein tyrosine phosphorylation is linked to cellular signaling processes that in turn control a host of fundamental cellular functions, including growth, differentiation, metabolism, progression through the cell cycle, migration, apoptosis/survival, and immune response.[1] The level of protein tyrosine phosphorylation is regulated by the action of protein−tyrosine kinases (PTKs) and protein−tyrosine phosphatases (PTPs). Perturbation of the balance between these enzymes disrupts cell function and has been implicated in a variety of disease states, including diabetes, obesity, and cancer.[2,3] Consequently, cellular pathways regulated by tyrosine phosphorylation offer a rich source of key targets for developing novel therapeutics.[4,5] The potential of such targeted therapeutics has been well-demonstrated by the successful treatment of human chronic myelogenous leukemia and gastrointestinal stromal tumors with the PTK inhibitor Gleevec,[6,7] which targets Bcr/Abl or c-kit aberrantly activated in the malignancies.

As observed with the PTKs, deregulation of PTP activity also contributes to the pathogenesis of a number of human diseases.[8,9] Since no formal functional linkage exists between the PTKs and PTPs, any single PTP could catalyze the dephosphorylation of proteins phosphorylated by more than one PTK. Thus, inhibitors of the PTPs are expected to have therapeutic value with unique modes of action. However, therapeutics based on PTPs were not seriously considered until recently. Progress in this area was initially stifled by the fact that the active site (i.e., pTyr binding site) is highly conserved among the large number of PTPs, making it difficult to achieve inhibitor selectivity. Fortunately, PTP substrate specificity studies have shown that pTyr alone is not sufficient for high-affinity binding, and residues flanking the pTyr are important for PTP substrate recognition.[10] These results suggest that unique PTP sub-pockets that border the active site may be targeted to enhance inhibitor affinity and selectivity. Major efforts have been made to develop nonhydrolyzable pTyr surrogates aimed to occupy the PTP active site.[11,12] The most useful and potent pTyr surrogate thus far devised for PTPs is phosphonodifluoromethyl phenylalanine (F_2Pmp).[13,14] Although F_2Pmp likely interacts in the desired inhibitory fashion with all PTPs, the molecular scaffolds to which the difluorophosphonate is attached should render the inhibitors PTP selective. Indeed, a number of potent and selective difluorophosphonate-based PTP1B inhibitors have been described.[15−17]

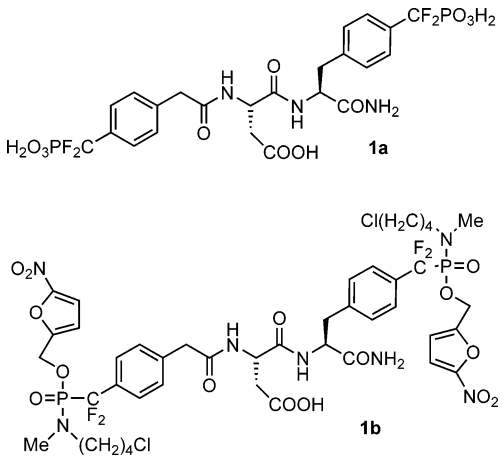

Figure 1. Structures of PTP1B inhibitor **1a** and its prodrug **1b**.

PTP1B is implicated as a key negative regulator of insulin and leptin signaling. In two landmark papers, it was shown that PTP1B deficient mice are more sensitive to insulin, have improved glycemic control, and are resistant to diet induced obesity.[18,19] The phenotype of PTP1B knockout mice suggests that an inhibitor of this PTP may address both obesity and insulin resistance, thereby presenting a unique therapeutic opportunity. Understandably, PTP1B is highly coveted by the pharmaceutical industry and constitutes a first example of a PTP with a physiological function that makes it an ideal drug target for therapeutic intervention in very common human diseases, type II diabetes and obesity.[20]

The most potent and selective PTP1B inhibitor reported is compound **1a** (Figure 1), which features an F_2Pmp residue linked to a second aryl difluorophosphonate group.[15] At physi-

* Corresponding author. Tel.: (765) 494-1403; fax (765) 494-1414; e-mail: borch@purdue.edu.
[†] Purdue University.
[‡] Indiana University School of Medicine.

10.1021/jm061146x CCC: $37.00
Published on Web 01/24/2007

Scheme 1

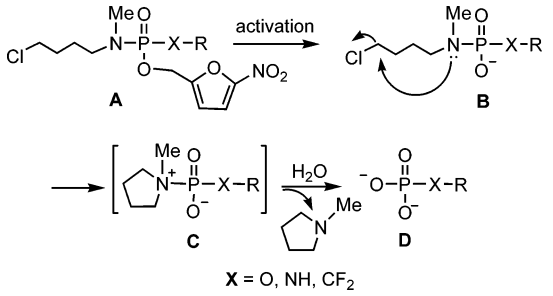

ologic pH, compound **1a** would be expected to be highly ionized and have exceedingly low membrane permeability. Indeed, compound **1a** is not cell permeable and exhibits no cellular activity.[21] To enhance penetration across the cell membrane, cell permeable derivatives of **1a** were prepared by coupling it to either the cell penetrating peptide (D)-Arg_8 via a disulfide bridge[22] or to a highly lipophilic fatty acid.[21] While these cell permeable analogues have enabled important validation of PTP1B as a therapeutic target and delineation of the roles of PTP1B in various signaling pathways,[21−24] they are unlikely to be suitable for the ultimate development of useful therapeutic agents.

Since a number of organophosphonate-based prodrugs have advanced to the clinic and beyond,[25] we sought to apply a prodrug strategy to improve the in vivo efficacy of compound **1a**. Previous attempts to improve cellular delivery of SH2 domain targeted peptides with phosphonate ester prodrugs have yielded very limited success.[26] Our laboratory has developed a novel prodrug approach that has been applied to the intracellular delivery of nucleotides and aryl phosphates.[27−29] Given the large number (5) of negative charges at physiologic pH, inhibitor **1a** represents an interesting challenge for prodrug delivery. We have extended our prodrug technology to investigate the synthesis and activation of difluoromethyl phosphonate prodrugs and the synthesis of prodrug **1b**. Studies with **1b** in a cell-based system indicate that our prodrug strategy provides an excellent solution to the drug delivery problem associated with organophosphonate-based PTP inhibitors.

Results and Discussion

Chemistry. The prodrug strategy is outlined in Scheme 1. The nitrofurfuryl delivery group in prodrug **A** imparts lipophilicity to enhance uptake into the cell. Once in the cell, the molecule undergoes sequential enzymatic reduction of the nitrofurfuryl group and cleavage to yield phosphonamidate **B**. The nitrogen can now participate in an intramolecular cyclization resulting in intermediate **C**, which hydrolyzes spontaneously to deliver the phosphorylated drug. The efficacy of this approach has been demonstrated for X = O and X =NH, but the effect of a difluoromethyl moiety (X = CF_2) on the prodrug strategy was unknown. Therefore, a model study was carried out initially to assess the synthetic approach and the activation process on a representative difluoromethyl analogue.

Model Studies. Compounds **4a** and **4b** were synthesized as shown in Scheme 2. Synthesis of **4a** allowed development of methods necessary to install the masking and delivery groups onto a difluoromethylphosphonate framework. Compound **4b** would provide the necessary precursor for chemical kinetic studies that would demonstrate the viability of the difluoromethyl group in prodrug activation. Arbuzov reaction of benzoyl chloride with triethylphosphite[30] followed by fluorination of the ketophosphonate by treatment with excess diethylaminosulfur

Scheme 2[a]

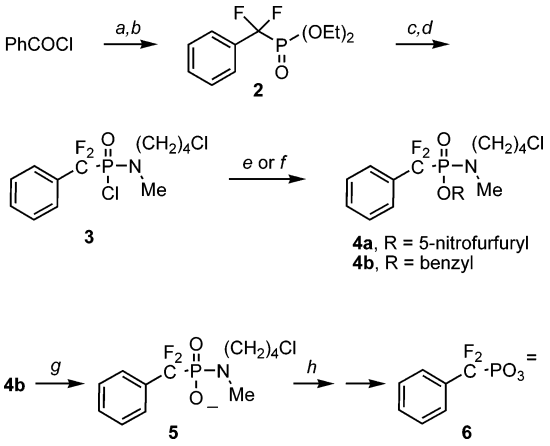

[a] Reagents and conditions: (a) $P(OEt)_3$, $CHCl_3$; (b) diethylaminosulfur trifluoride, 0 °C to rt, 20 h; (c) $SOCl_2$, DMF (cat); (d) $CH_3NH(CH_2)_4Cl$·HCl, DIEA, CH_2Cl_2, −20 °C; (e) nitrofurfuryl alcohol, LiHMDS, THF, −78 °C; (f) BnOH, *n*-BuLi, −78 to −40 °C, 3 h; (g) H_2, Pd-C; and (h) cacodylate buffer, pH 8.5, 37 °C.

trifluoride (DAST)[31] afforded difluoromethylphosphonate **2**. This compound was refluxed with thionyl chloride to generate the labile phosphonyl dichloride, which was used without further purification. Sequential addition of *N*-methyl-*N*-(4-chlorobutyl)-amine to give monochloride **3** followed by reaction with the lithium salts of the appropriate alcohols gave compounds **4a** and **4b** in good overall yields.

^{31}P NMR Kinetics Study. The intracellular activation of prodrug **4a** can be modeled in vitro by catalytic hydrogenolysis of benzyl ester **4b**. Thus, **4b** was subjected to hydrogenolysis resulting in its quantitative conversion to phosphonamidate anion **5** (as determined by ^{31}P NMR). This anion was immediately taken up in 0.4 M cacodylate buffer/CH_3CN, and its conversion to difluoromethylphosphonate **6** (Scheme 2) was monitored by ^{31}P NMR at 37 °C over 2 h. The ^{31}P triplet at −15 ppm corresponding to phosphonamidate **5** slowly disappeared and was replaced by a new triplet at −20 ppm corresponding to the phosphonate **6**; this conversion proceeds with a half-life ($t_{1/2}$) of 44 min. This contrasts with $t_{1/2}$ values of 2−21 min (T = 37 °C, pH = 7.2−7.4) for phosphoramidate analogues (X = O or NH, Scheme 1).[28,29] It is not unexpected that the strongly electron-withdrawing CF_2 group retards the cyclization of the difluoromethylphosphonamidate **5**. The $t_{1/2}$ of 44 min under model physiologic conditions is not pharmacologically prohibitive for phosphonate delivery, so our attention was directed to the synthesis of **1b**.

Target Molecule Synthesis. Construction of **1b** requires the synthesis of two prodrug building blocks **11**, derived from 4-iodophenylacetic acid, and **12b**, derived from *N*-Fmoc-(L)-4-iodophenylalanine. Scheme 3 details installation of the difluoromethylphosphonate ester moiety into the corresponding aromatic precursors. Copper-catalyzed coupling of aryl iodides **7a** and **7b** with the organocadmium reagent derived from diethyl bromodifluoromethylphosphonate as described by Qabar[32] provided diethyl difluoromethylphosphonates **8a** and **8b** in good yields. Conversion of the phosphonate esters to the reactive phosphonyl dichlorides was accomplished by reaction with TMSBr and treatment of the resulting silyl phosphonate intermediate with oxalyl chloride.[33] This procedure was a vast improvement over the prolonged reaction with thionyl chloride utilized for the synthesis of the model compounds (Scheme 2). Installation of the masking and delivery groups as described for the synthesis of **4a** provided the ester protected prodrugs

Scheme 3[a]

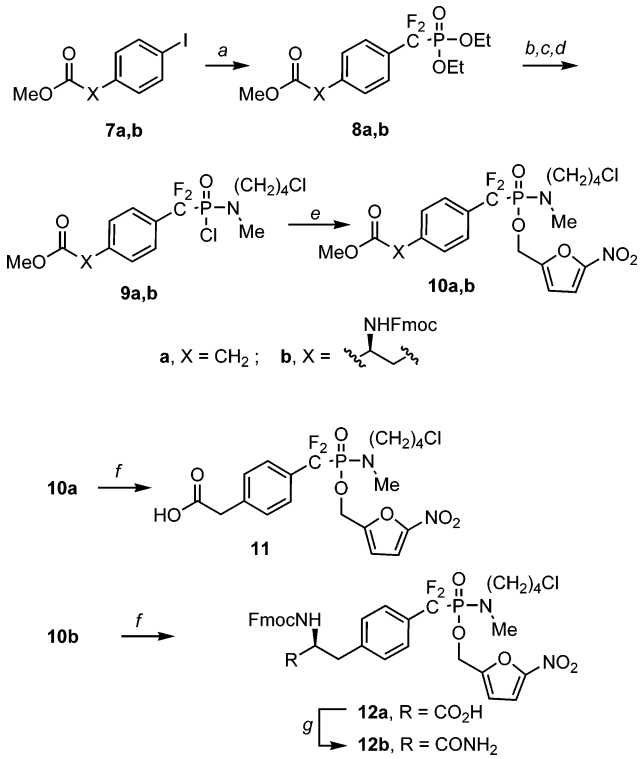

[a] Reagents and conditions: (a) Cd, $BrCF_2P(O)(OEt)_2$, TMSCl, CuCl; (b) TMSBr, CH_2Cl_2; (c) oxalyl chloride, CH_2Cl_2; (d) $CH_3NH(CH_2)_4Cl$·HCl, DIEA, CH_2Cl_2, −20 °C; (e) nitrofurfuryl alcohol, LiHMDS, THF, −78 °C; (f) Me_2SnOH, DCE, 80 °C; and (g) DIC, NHS, NH_4HCO_3, THF.

10a and **10b**. Selective hydrolysis of the methyl esters proved to be problematic. Standard lithium hydroxide hydrolysis at 0 °C resulted in decomposition. Alternative reagents such as $(NH_4)_2CO_3$, K_2CO_3, $Ba(OH)_2$, and Cs_2CO_3 resulted either in recovery of starting ester or in decomposition. Other ester groups were investigated to no avail. Surprisingly, treatment of the benzyl ester analogue corresponding to **10b** with TMSI resulted in clean removal of the nitrofurfuryl group, leaving the benzyl ester intact. Attempts to cleave either the methyl or the benzyl esters via enzymatic hydrolysis resulted in recovery of the starting material. Attempted deprotection of the phenacyl ester analogue of **10b**[34] resulted in decomposition as well. Reaction of the propargyl ester analogue of **10b** with tributyltin hydride appeared to be effective but was not reproducible. Protecting groups such as allyl and 2,4-dimethoxybenzyl did not survive the reaction with TMSBr and could not be employed. Ultimately, it was found that lithium hydroxide added carefully in small increments over short reaction times led to methyl ester hydrolysis providing the desired acids. Subsequently, it was discovered that reaction with trimethyltin hydroxide[35] in DCE at 80 °C provided the free acids cleanly. This method is reported to avoid epimerization sometimes experienced with LiOH and is compatible with many commonly used protecting groups. To confirm that chiral integrity was preserved throughout the esterification and de-esterification reactions, methyl ester **7b** was subjected to hydrolysis by both the LiOH and the Me_3SnOH methods. The carboxylic acids obtained were analyzed on a chiral HPLC column and were compared to authentic samples of (L)- and (D)-*N*-Fmoc-iodophenylalanine. No trace of (D)-amino acid was observed from either hydrolysis process. Finally, the Fmoc protected amino acid was converted to the primary amide using standard NHS-carbodiimide coupling chemistry.

Scheme 4[a]

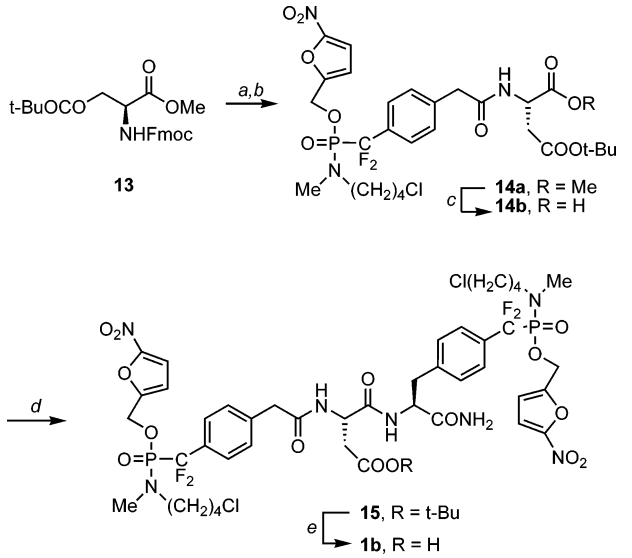

[a] Reagents and conditions: (a) DBU/CH_2Cl_2; (b) **11**, PyBOP, DIEA, CH_2Cl_2; (c) LiOH/H_2O, THF, 0 °C; (d) **12b** + DBU/CH_2Cl_2, then PyBOP, DIEA, CH_2Cl_2; and (e) TFA/CH_2Cl_2.

With the two requisite building blocks **11** and **12b** in hand, the target molecule was then assembled. The main challenge was to retain the somewhat labile nitrofurfuryl groups during the two required Fmoc deprotections. Brief exposure to DBU in CH_2Cl_2 at 0 °C with careful TLC monitoring effected removal of the Fmoc group without modification of the nitrofurfuryl group. Although solid phase synthesis can be used in the construction of **1b,** the inability to monitor Fmoc deprotection, the strongly acidic conditions required for cleavage from the resin, and the potential need for scaleup synthesis led us to pursue a solution phase approach for the synthesis of acyl dipeptide **1b**.

The convergent synthesis of **1b** is outlined in Scheme 4. Protected aspartate **13** was deprotected by treatment with DBU/CH_2Cl_2 at 0 °C for 25 min. The resulting aminoester was coupled to **11** using PyBOP/DIEA to yield acyl aspartate **14a** in 65% yield. The methyl ester group of **14a** was hydrolyzed using LiOH/H_2O to give the corresponding carboxylic acid **14b** in 68% yield. Compound **12b** was treated with DBU/CH_2Cl_2 at 0 °C to remove the Fmoc group, and coupling of the resulting amino amide to **14b** was achieved in 47% yield using PyBOP and DIEA. Finally, the *t*-butyl ester moiety of **15** was hydrolyzed with TFA/CH_2Cl_2 to give the desired acyldipeptide prodrug **1b** in 82% yield.

Biological Evaluation. Compound **1a** displays a K_i value of 2.4 nM for PTP1B and exhibits several orders of magnitude of selectivity in favor of PTP1B against a panel of PTPs.[15] The negatively charged difluorophosphonate functional groups in compound **1a** participate in key active site and near active site interactions that are responsible for the high PTP1B potency and selectivity displayed by **1a**.[36,37] Masking the negative charges in the difluorophosphonate groups would lead to a decrease in inhibitory activity of compound **1a**. As expected, the prodrug **1b** did not exhibit significant inhibition of the PTP1B-catalyzed reaction even at concentrations as high as 20 μM, a nearly 4 orders of magnitude loss in activity in comparison with the unmodified **1a**. We predict that, upon entry inside the cell, the prodrug will undergo sequential enzymatic and spontaneous chemical transformation, regenerating the PTP1B inhibitory species **1a**.

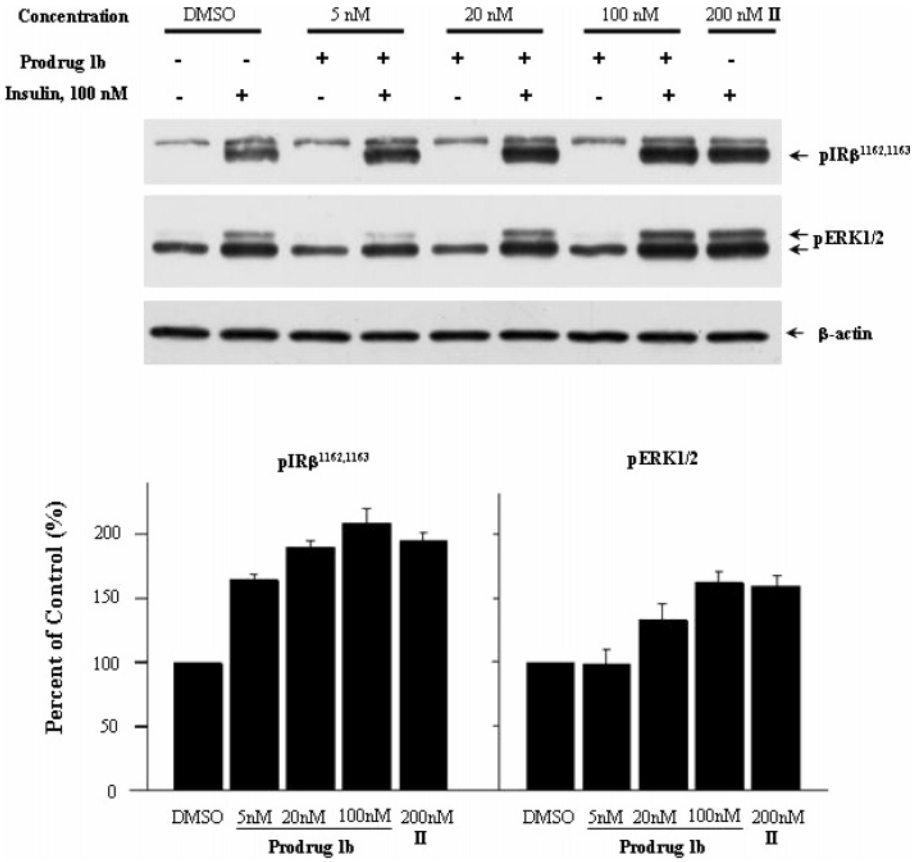

Figure 2. Concentration dependence of prodrug **1b** on insulin signaling in HepG2 cells. Subconfluent HepG2 cells were treated with a range of concentrations of prodrug **1b** (0, 5, 20, and 100 nM) or 200 nM of the cell permeable fatty acid conjugated derivative of **1a** (compound **II**[21]) for 1 h, which was followed by a 5 min treatment with (lanes 2, 4, 6, and 8) or without (lanes 1, 3, 5, 7, and 9) 100 nM insulin. Cell lysates were subjected to SDS-PAGE, and the resolved proteins were transferred to nitrocellulose membranes, which were blocked with anti-phospho-IRβ and anti-phospho-ERK1/2 antibodies. β-Actin was used as a loading control.

Insulin mediated activation of the insulin receptor (IR) produces a wide array of cellular responses, including enhanced phosphorylation of the insulin receptor β (IRβ) subunit and the extracellular signal regulated protein kinase 1 and 2 (ERK1/2).[38,39] Previous studies have demonstrated that PTP1B serves as a negative regulator of the insulin activated signaling pathways by catalyzing the dephosphorylation of IRβ. Consequently, inhibition of PTP1B activity should enhance insulin signaling. For example, IRβ phosphorylation in the liver of the PTP1B knockout mice is prolonged 2-fold.[18,19] The antisense mediated reduction of PTP1B in rat hepatoma cells generates a 2.3-fold increase in the phosphorylated IRβ level.[40] In addition, significant enhancements in IRβ phosphotyrosine levels have been reported with a fatty acid conjugated derivative of **1a** (identified as compound **II** in Figure 2).[21]

To assess the efficacy of the prodrug delivery strategy, we determined the cellular effects of compound **1b** on insulin signaling in human hepatoma HepG2 cells. The cells were exposed to prodrug **1b** over a selected range of concentrations for 1 h and subsequently treated either with or without insulin (100 nM) for 5 min. Cell lysates were resolved by SDS-PAGE and the resolved proteins were transferred to nitrocellulose membranes and probed with both anti-phospho-IRβ (pY1162/pY1163) and anti-phospho-ERK1/2 antibodies. As shown in Figure 2, prodrug **1b** can increase the insulin induced activation of both IRβ and its downstream targets ERK1/2. The maximal effect of **1b** in HepG2 cells appears to peak around 20 nM. At 20 nM ($\sim$8$\times$ the K_i of **1a** for PTP1B), prodrug **1b** enhanced the phosphorylation levels of IRβ and ERK1/2 by 1.9- and 1.3-fold, respectively. A somewhat more pronounced effect was observed at 100 nM **1b** (2.1- and 1.6-fold increase for IRβ and ERK1/2, respectively). As a positive control, treatment of the HepG2 cells with a known cell permeable fatty acid conjugated **1a** derivative (compound **II** in Figure 2) (K_i = 26 nM for PTP1B) led to similar increases in IRβ and ERK1/2 phosphorylation (2- and 1.6-fold, respectively) at a concentration of 200 nM ($\sim$8$\times$ the K_i) (Figure 2). These results suggest that the prodrug strategy is very effective in promoting cellular uptake of difluoromethyl phosphonates and that the liberated PTP1B inhibitor has ready access to the cytoplasmically oriented protein target.

To investigate how fast it would take the prodrug to exert its biological effect, HepG2 cells pretreated with 20 nM prodrug **1b** for various time intervals were stimulated with or without 100 nM insulin for 5 min. As shown in Figure 3, a 35% increase in the insulin induced IRβ phosphorylation was observed when the cells were pretreated with the prodrug for only 5 min. Preincubation of the cells with the prodrug for 20 and 60 min generated 1.7- and 2-fold increases in the insulin induced IRβ phosphorylation, while the ERK1/2 phosphorylation was increased by 25 and 50%, respectively. Prolonged incubation (2 h) with 20 nM prodrug only led to a modest increase in cellular activity (a 2.1-fold increase in IRβ phosphorylation and no further increase in ERK1/2 phosphorylation) (data not shown). These results are in general agreement with the observed conversion half-life ($t_{1/2}$) of 44 min for model prodrug **4b** in solution. The fact that the biological effects produced by the prodrug at a concentration only a few times over its K_i are identical to those observed in PTP1B deficient mice, cells treated with PTP1B antisense oligo, or a cell permeable PTP1B inhibitor

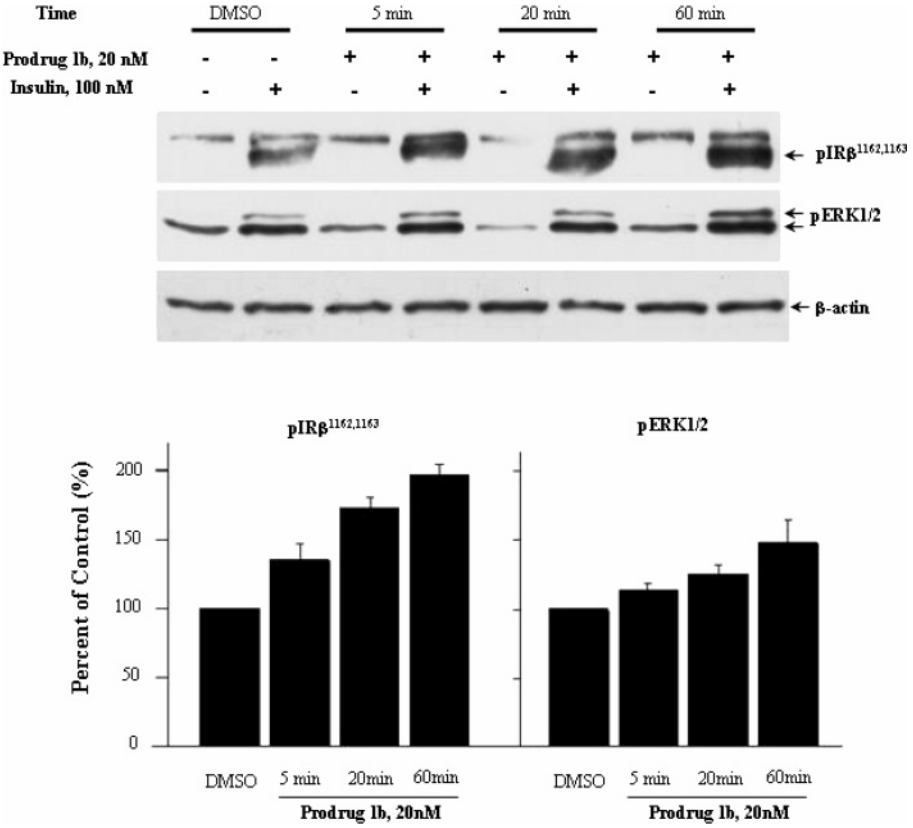

Figure 3. Time course of prodrug **1b** delivery. Subconfluent HepG2 cells were preincubated with 20 nM prodrug **1b** for various amounts of time. Subsequently, the cells were stimulated without (lanes 1, 3, 5, and 7) or with (lanes 2, 4, 6, and 8) 100 nM insulin for 5 min. Cell lysates were subjected to SDS-PAGE, and the resolved proteins were transferred to nitrocellulose membranes, which were blocked with anti-phospho-IRβ and anti-phospho-ERK1/2 antibodies. β-Actin was used as a loading control.

indicates that the conversion of the prodrug **1b** to PTP1B inhibitor **1a** is nearly complete in the cellular environment.

Conclusion

We have extended our prodrug technology to investigate the synthesis and activation of difluoromethyl phosphonates and the synthesis of PTP1B prodrug **1b**. Studies with **1b** in human HepG2 cells indicate that our prodrug strategy provides an excellent solution to the drug delivery problem associated with organophosphonate-based PTP inhibitors. The cell-based studies in this paper show that prodrug **1b** can potentiate the insulin signaling pathway. Future studies will assess the utility of prodrug **1b** for the treatment of diabetes and obesity.

Experimental Procedures

Materials and Methods. All NMR spectra were recorded using a 300 MHz Bruker spectrometer equipped with a 5 mm multinuclear probe unless otherwise specified. ^{1}H chemical shifts are reported in parts per million from tetramethylsilane unless otherwise specified. ^{31}P NMR spectra were obtained using broadband ^{1}H decoupling, and chemical shifts are reported in parts per million using 1% triphenylphosphine oxide/benzene-d_6 as the coaxial reference (triphenylphosphine oxide/toluene-d_8 has a chemical shift of +24.7 ppm relative to 85% phosphoric acid). Variable temperature ^{31}P NMR kinetics experiments were controlled using the variable temperature unit of a Bruker 250 MHz spectrometer. Multiplicities of ^{13}C NMR peaks of **1b** were determined from DEPT experiments employing standard pulse sequences. HPLC analysis was done using a Beckman System Gold equipped with a 168 detector set at 310 nm, a 126 solvent module, and Econosphere C18 and phenyl columns from Alltech Associates. A normal-phase Chiralcel OD column from Daicel Chemical Industries (OD00CE-FF028) was also employed. Mass spectral analysis was obtained from the mass spectrometry laboratory at Purdue University, West Lafayette, IN.

All anhydrous reactions were carried out under an atmosphere of argon. All organic solvents were distilled prior to use unless otherwise specified. Flash chromatography using silica gel grade 60 (230−400 mesh) was carried out for all chromatographic separations. Thin layer chromatography was performed using Analtech glass plates precoated with silica gel (250 nm). Visualization of the plates was accomplished using UV and/or Hanessian's Stain (5.0 g of $Ce(SO_4)_2$, 25.0 g of $(NH_4)Mo_7)_{24}\cdot 4H_2O$, 450 mL of H_2O, and 50 mL of H_2SO_4) followed by heating.

Antibodies and Chemicals. Polyclonal insulin receptor (IR) β subunit dual-phospho-specific (pYpY1162/1163) antibody was purchased from BioSource International (Camarillo, CA); polyclonal anti-phospho-ERK1/2 antibody, secondary anti-mouse, as well as anti-rabbit IgG(H + L) conjugated with HRP were obtained from Cell Signaling Technology. Human insulin, sodium orthovanadate, iodoacetic acid, and Nonidet P-40 were from Sigma (St. Louis, MO).

Cell Lines and Tissue Culture. The human hepatoma cells (HepG2) were obtained from ATCC (HB-8065). HepG2 cells were grown and maintained in Minimum Essential Medium (MEM, Eagle) with 2 mM L-glutamine, 1 mM sodium pyruvate, and 10% fetal bovine serum in a 5% CO_2 environment.

Immunoblotting. The 60−80% confluent HepG2 cells were starved for 5 h in MEM without serum. Then, cells were treated for 1 h with a range of concentrations of prodrug **1b**, followed by stimulation with or without 100 nM insulin for 5 min. The incubation was terminated by removing the fluid, and the cells were washed by cold PBS. Cells were scraped and lysed with the lysis buffer (50 mM Tris-HCl, pH 7.5, 150 mM NaCl, 1% NP-40, 10 mM sodium pyrophosphate, 5 mM iodoacetic acid, 10 mM NaF, 1 mM EDTA, 2 mM orthovanadate, 5 mg/mL leupeptin, 5 mg/mL aprotinin, 0.1 mg/mL PMSF, and 1 mM benzamidine). After 30

min lysing on ice, the cell lysate was centrifuged at 15 000 rpm for 15 min. The total cellular proteins were separated by SDS-PAGE and transferred electrophoretically to nitrocellulose membranes, which were then immunoblotted by anti-phospho-IRβ or anti-phospho-ERK1/2 antibodies. To control for equal sample loading, the membrane was also probed with anti-actin antibody. The blots were developed using the Western blot detection kit (Upstate) according to the manufacturer's instructions. Western blotting images were analyzed with Image J (NIH).

In Vitro Inhibition Studies with Prodrug 1b. IC_{50} values for prodrug **1b** were determined for PTP1B in the following manner. At fixed substrate *p*-nitrophenyl phosphate (pNPP) concentration (2 mM at the K_m), the initial rate at various **1b** concentrations was measured by following the production of *p*-nitrophenol as described.[36] All experiments were performed at 30 °C in 50 mM 3,3-dimethylglutarate buffer, pH 7.0, containing 1 mM EDTA with an ionic strength of 0.15 M adjusted with NaCl.

^{31}P NMR Kinetics. A ^{31}P NMR kinetics experiment was carried out at 37 °C on a 250 MHz Bruker NMR using the Bruker variable temperature unit to control the probe temperature. Compound **4b** (7.7 mg, 0.021 mmol) in 1 mL of THF was treated with a suspension of Pd/C, 10% (5 mg), in 1 mL of THF. A balloon filled with H_2 was applied to the flask. After 5 min, the suspension was filtered through two pieces of filter paper, and the filtrate was concentrated until the solvent had just evaporated (bath $T = 30$ °C). Sodium cacodylate buffer (0.4 M, 0.5 mL) was added to the resulting oil, and the time of dilution was noted. Triethylamine (0.5 mL) was added to adjust the pH to 7.68, and the sample was immediately inserted into the spectrometer. The elapsed time from addition of buffer was noted at the start of acquisition. Spectra were acquired every 2.5 min for 30 min, then every 5 min for 30 min and every 10 min for 1 h. A pH of 7.14 was recorded at the end of the experiment. The relative concentrations of reaction intermediates were determined by measuring the peak areas, and the relative concentration for each reactant or product at any given time is represented as a percent of the total. The phosphonamidate anion derived from **4b** disappeared according to first-order kinetics, and the half-life ($t_{1/2}$) was determined to be 44 min at 37 °C by linear regression of the log(percent remaining) values versus time.

Diethyl Difluoromethylbenzylphosphonate (2). The procedure of Burke and co-workers[31] was used. Diethyl benzoylphosphonate (2.58 g, 10.65 mmol), prepared from benzoyl chloride and triethyl phosphate as described,[30] and (diethylamino)sulfur trifluoride (DAST) (6.0 mL, 45.41 mmol, 4.3 equiv) were stirred together at 0 °C under an Ar atmosphere. The reaction was warmed to ambient temperature over 1 h and continued to stir for 20 h. The reaction mixture was then rechilled to 0 °C and added to a 25% solution of $NaHCO_3$ in H_2O (100 mL) cooled to 0 °C. The resulting suspension was stirred for 15 min, 150 mL of H_2O was added, and the aqueous phase was extracted with four 50 mL portions of $CHCl_3$. The combined organic extracts were washed with brine, dried over Na_2SO_4, and concentrated to a brown oil. The crude material was purified by flash column chromatography using 10% EtOAc/hexane. The product **2** was isolated (1.18 g, 42%) as an amber oil $R_f = 0.23$, 20% EtOAc/hexane. ^{1}H NMR ($CDCl_3$): δ 7.62 (2H, d) 7.45 (3H, m) 4.22−4.12 (4H, m) 1.30 (6H, t); ^{31}P NMR ($CDCl_3$) δ −19.07 (t); HRMS ($C_{11}H_{15}F_2O_3P$) calcd 265.0805, found 265.0802.

***N*-Methyl-*N*-(4-chlorobutyl) Difluoromethylphenylphosphonamidochloridate (3).** Compound **2** (0.25 g, 0.95 mmol) was dissolved in thionyl chloride (5 mL), three drops of pyridine were added, and the mixture was refluxed under an atmosphere of Ar for 5 days at which time TLC (10% EtOAc/hexane) showed no starting material remaining. Thionyl chloride was removed under reduced pressure to give the corresponding dichloride (^{31}P NMR ($CDCl_3$) δ +5.93 (t)), which was taken up in dry CH_2Cl_2 (12 mL) and was cooled to −78 °C with stirring under an Ar atmosphere. *N*-Methyl-*N*-(4-chlorobutyl)amine hydrochloride (0.14 g, 0.89 mmol, 0.94 equiv) was added followed by triethylamine (0.27 mL, 1.94 mmol, 2.0 equiv). The reaction was maintained at −78 °C for 20 h. Solvent was removed under reduced pressure, and the residue was purified by flash column chromatography using 10% EtOAc/hexane as eluent to provide **3** (0.18 g, 57%) as a pale yellow oil. $R_f = 0.33$, 20% EtOAc/hexane. ^{1}H NMR ($CDCl_3$): δ 7.62 (2H, d); 7.54−7.45 (3H, m); 3.48 (2H, t); 3.21−3.03 (2H, m); 2.80 (3H, d); 1.71−1.54 (4H, m); ^{31}P NMR ($CDCl_3$) δ +3.40 (t); HRMS ($C_{12}H_{16}Cl_2F_2NOP$) calcd 330.0393, found 330.0403 .

***O*-Nitrofurfuryl *N*-Methyl-*N*-(4-chlorobutyl) Difluoromethylphenylphosphonamidate (4a).** 5-Nitrofurfuryl alcohol (0.05 g, 0.35 mmol, 1.1 equiv) and 4-(phenylazo)diphenylamine (3 mg) in THF (2.2 mL) was cooled to −78 °C with stirring under an Ar atmosphere. A 1.0 M solution of lithium bis(trimethylsilyl)amide was added dropwise via syringe until the color of the reaction mixture changed from orange to violet. This required 0.41 mL (0.41 mmol, 1.2 equiv) of base. This mixture was stirred at −78 °C for 15 min while a solution of **3** (0.11 g, 0.34 mmol, 1 equiv) in THF (2.2 mL) under an Ar atmosphere was prepared and cooled to −78 °C. The alkoxide solution was transferred rapidly by cannula to the solution of **3**, and the resulting mixture was maintained at −78 °C for 10 h. The reaction mixture was quenched with 5 mL of saturated NH_4Cl solution, and the aqueous phase was extracted 3 times with Et_2O (10 mL each). The combined organic extracts were washed with brine, dried over Na_2SO_4, and concentrated to an amber oil. The crude material was purified by flash column chromatography using gradient elution (25%, 50% EtOAc/hexane) to provide **4a** (0.13 g, 88%) as a light amber oil. $R_f = 0.31$, 50% EtOAc/hexane. ^{1}H NMR ($CDCl_3$): δ 7.55 (2H, d); 7.42 (3H, m); 7.20 (1H, d); 6.53 (1H, d); 5.00 (2H, m); 3.49 (2H, t); 2.95 (2H, m) 2.65 (3H, d); 1.71−1.56 (4H, m); ^{31}P NMR ($CDCl_3$) δ −10.40 (dd); HRMS ($C_{17}H_{20}ClF_2N_2O_5P$) calcd 459.0664 $(M + Na)^+$, found 459.0664.

***O*-Benzyl *N*-Methyl-*N*-(4-chlorobutyl) Difluoromethylphenylphosphonamidate (4b).** Compound **4b** was obtained in 70% yield using the procedure described for the synthesis of **4a**. Benzyl alcohol was substituted for nitrofurfuryl alcohol, and BuLi was used instead of lithium bis(trimethylsilyl)amide. The crude product was purified by flash column chromatography (10% EtOAc/hexane) to give **4b** (0.090 g, 70%), $R_f = 0.54$, 50% EtOAc/hexane. ^{1}H NMR ($CDCl_3$): δ 7.59 (2H, d); 7.42 (3H, m); 7.30 (5H, m); 5.03 (2H, d); 3.47 (2H, t); 2.99 (2H, m); 2.62 (3H, d); 1.67−1.48 (4H, m); ^{31}P NMR ($CDCl_3$): δ −11.32 (dd); HRMS ($C_{19}H_{23}ClF_2NO_2P$) calcd 402.1201, found 402.1202.

Methyl 4-Iodophenylacetate (7a). 4-Iodophenylacetic acid (5.56 g, 22.06 mmol) was suspended in MeOH (35 mL) and stirred under a drying tube at 0 °C. Thionyl chloride (3.20 mL, 43.84 mmol, 2 equiv) was added by addition funnel. The reaction came gradually to room temperature and was stirred overnight. The solution was then concentrated to ca. half of its initial volume, diluted with 50 mL of EtOAc, and washed successively with 25 mL portions of H_2O, saturated $NaHCO_3$ solution, and brine. Concentration after drying over Na_2SO_4 gave **7a** (5.79 g, 95%) as a yellow oil with spectral data that were consistent with literature values.[40] The product was used without purification. $R_f = 0.13$, 15% EtOAc/hexane.

Methyl *N*-Fmoc-(L)-4-iodophenylalaninate (7b). Compound **7b** (9.84 g, 96%) was obtained as a white solid using the procedure described for compound **7a** and was used without further purification. Spectral data were consistent with published values. $R_f = 0.23$, 20% EtOAc/hexane.

Methyl 4-[(Diethyl Phosphono(difluoromethyl)]phenylacetate (8a). The procedure of Qabar[32] with a slight modification was employed as follows. Cadmium powder (7.5 g, 66.7 mmol, 3.2 equiv) in 74 mL of DMF was treated with TMSCl (0.27 mL, 2.12 mmol, 0.1 equiv). After 5 min, diethyl (bromodifluoromethyl)-phosphonate (11.5 mL, 64.7 mmol, 3.1 equiv) was added dropwise from an addition funnel. The reaction mixture became warm and cloudy. If no exothermicity was observed after adding approximately one-third of the phosphonate, an additional portion of chlorotrimethylsilane was added before continuation of the addition of phosphonate. Formation of $BrCdCF_2P(O)(OEt)_2$ was deemed complete by the absence of starting phosphonate (TLC, 15% EtOAc/hexane). Aryl iodide **7a** (5.79 g, 21.0 mmol, 1 equiv) and CuCl (8.3 g, 83.8 mmol, 4 equiv) were suspended in 17 mL of DMF. To

this suspension, the organocadmium reagent was added by cannula. The resulting mixture was stirred under Ar at room temperature for 4 days. The reaction was diluted with 75 mL of Et_2O and filtered through celite. The filtrate was washed with brine, dried over Na_2SO_4, and concentrated to a gold oil. The oil was subjected to Kugelrohr distillation at reduced pressure (1.5 Torr, 80 °C) to remove volatile byproducts. Compound **8a** (6.40 g, 91%) was obtained from the distillation bulb as a yellow oil and was used without further purification. $R_f = 0.37$, 5% Et_2O/CH_2Cl_2. ^1H NMR ($CDCl_3$): δ 7.56 (2H, d); 7.37 (2H, d); 4.18 (4H,m); 3.70 (3H, s); 3.66 (2H, s); 1.33 (6H, t); ^{31}P NMR ($CDCl_3$): δ −19.20 (t); HRMS ($C_{14}H_{19}F_2O_5P$) calcd 336.0938, found 336.0938.

Methyl 4-[(Diethyl Phosphono(difluoromethyl)]-*N*-Fmoc-(L)-phenylalaninate (8b). The procedure utilized for the synthesis of **8a** was employed to prepare **8b** (4.92 g, 80%). Purification was effected by Kugelrohr distillation (80 °C, 1.55 Torr) to remove volatile side products. The remaining oil was further purified by flash column chromatography (gradient elution: 0, 20, 50% EtOAc/hexane). $R_f = 0.31$, 10% Et_2O/CH_2Cl_2. Spectral data were consistent with published values.[32]

Methyl 4-[Chloro-*N*-methyl-*N*-(4-chlorobutyl) Phosphono-(difluoromethyl)]phenylacetate (9a). The procedure of Landry and co-workers[13] was used to activate diethylphosphonate **8a**. Thus, **8a** (3.02 g, 8.98 mmol) in 70 mL of dry CH_2Cl_2 was treated with bromotrimethylsilane (3.50 mL, 26.5 mmol, 3 equiv), and the mixture was stirred under a drying tube for 18 h. Solvent was removed under reduced pressure, and the residue was coevaporated with CH_2Cl_2 (2 × 30 mL) to remove excess bromotrimethylsilane. The resulting oil was taken up in CH_2Cl_2 (70 mL), and oxalyl chloride (2.40 mL, 27.4 mmol, 3 equiv) was added followed by 2 drops of dry DMF. The reaction mixture was stirred under an Ar atmosphere for 1.5 h, solvent was removed under reduced pressure, and the residue was coevaporated with CH_2Cl_2 (2 × 30 mL) to remove excess oxalyl chloride. The resulting oil was taken up in CH_2Cl_2 (70 mL) and was cooled to −20 °C with stirring under an Ar atmosphere. *N*-Methyl-*N*-(4-chlorobutyl)amine hydrochloride (1.56 g, 9.87 mmol, 1.1 equiv) was added followed by dropwise addition of diisopropylethylamine (3.40 mL, 19.5 mmol. 2.2 equiv). The reaction mixture was maintained at −20 °C for 20 h. Solvent was removed under reduced pressure, and the residue was purified by flash column chromatography using 3% Et_2O/CH_2Cl_2 as eluent providing **9a** (2.54 g, 70%) as a yellow oil. $R_f = 0.56$, 5% Et_2O/CH_2Cl_2. ^1H NMR ($CDCl_3$): δ 7.58 (2H, d); 7.40 (2H, d); 3.71 (3H, s); 3.68 (2H, s); 3.49 (2H, t); 3.25−3.02 (2H, m); 2.81 (3H, d); 1.72−1.52 (4H, m); ^{31}P NMR ($CDCl_3$): δ +3.99 (t); HRMS ($C_{15}H_{20}Cl_2F_2NO_3P$) calcd $(M + Na)^+$ 424.0418, found 424.0437.

Methyl 4-[Chloro *N*-Methyl-*N*-(4-chlorobutyl) Phosphono-(difluoromethyl)]-*N*-Fmoc-(L)-phenylalaninate (9b). The same procedure used for the synthesis of **9a** was employed to provide **9b** (2.89 g, 85%) after purification by flash column chromatography (2% Et_2O/CH_2Cl_2). R_f = 0.35, 5% Et_2O/CH_2Cl_2. ^1H NMR ($CDCl_3$): δ 7.75 (2H, d); 7.53 (4H, m); 7.40 (2H, t); 7.31 (2H, d); 7.22 (2H, d); 5.55 (1H, t); 4.66 (1H, m); 4.43−4.35 (2H, m); 4.19 (1H, t); 3.70 (3H, s); 3.46 (2H, t); 3.18−3.05 (4H, m); 2.75 (3H, dd); 1.62−1.44 (4H, m); ^{31}P NMR ($CDCl_3$): δ +3.95 (t); HRMS ($C_{31}H_{33}Cl_2F_2N_2O_5P$) calcd $(M + Na)^+$ 675.1370, found 675.1375.

Methyl 4-[*O*-Nitrofurfuryl *N*-Methyl-*N*-(4-chlorobutyl) Phosphono(difluoromethyl)] Phenylacetate (10a). Compound **10a** (4.11 g, 60%) was obtained using the same method employed in the synthesis of **4a**. The compound was purified by flash column chromatography using gradient elution (50%, 60% EtOAc/hexane). $R_f = 0.29$, 60% EtOAc/hexane. ^1H NMR ($CDCl_3$): δ 7.54 (2H, d); 7.36 (2H, d); 7.25 (1H, d); 6.54 (1H, d); 5.03 (2H, m); 3.72 (3H, s); 3.68 (2H, s); 3.54 (2H, t); 3.07 (2H, m); 2.72 (3H, d); 1.78−1.66 (4H, m); ^{31}P NMR ($CDCl_3$): δ −10.54 (t); HRMS ($C_{20}H_{24}ClF_2N_2O_7P$) calcd $(M + Na)^+$ 531.0875, found 531.0872.

Methyl 4-[*O*-Nitrofurfuryl *N*-Methyl-*N*-(4-chlorobutyl) Phosphono(difluoromethyl)]-*N*-Fmoc-(L)-phenylalaninate (10b). The procedure utilized for the synthesis of **4a** was applied to obtain **10b** (1.92 g, 41%) The compound was purified by flash column chromatography using gradient elution (30, 60, 80% Et_2O/hexane). $R_f = 0.50$, 70% EtOAc/hexane. ^1H NMR ($CDCl_3$): δ 7.72 (2H, d); 7.53−7.17 (11H, m); 6.50 (1H, bs); 5.02−4.87 (2H, m); 4.63 (1H, m); 4.35 (2H, m); 4.15 (1H, t); 3.68 (3H, s); 3.48 (2H, t); 3.16−2.98 (4H, m); 2.62 (3H, d); 1.68−1.53 (4H, m); ^{31}P NMR ($CDCl_3$): δ −10.50 (dd); HRMS ($C_{36}H_{37}ClF_2N_3O_9P$) calcd 782.1822 $(M + Na)^+$, found 782.1816.

General Procedure A: Methyl Ester Hydrolysis using LiOH. The methyl ester (0.35 mmol) in 5.5 mL of THF/H_2O (5:1) was cooled to 0 °C, and 0.3 M LiOH/H_2O (2 equiv) was added dropwise in the following increments: 1.1, 0.4, 0.4, and 0.4 mL. The reaction was monitored by TLC (2% MeOH, 1% AcOH/CH_2Cl_2) after each addition of base. The reaction was quenched with 10 mL of 10% citric acid 10 min after the final addition of base. The reaction mixture was extracted with EtOAc (4 × 10 mL), and the combined extracts were washed with brine, dried over Na_2SO_4, and concentrated to an oil that was purified by silica gel chromatography.

General Procedure B: Methyl Ester Hydrolysis using Me_3SnOH. The hydrolysis procedure of Nicolaou and co-workers[35] was employed. The methyl ester (0.05 mmol) was dissolved in 1,2-dichloroethane (1 mL), and Me_3SnOH (0.22 mmol, 4.4 equiv) was added. The reaction mixture was heated to reflux for 20 h at which time the disappearance of the starting material was observed by TLC (50% EtOAc/hexane). Solvent was removed under reduced pressure, and the residue was taken up in 5 mL of EtOAc. The solution was washed with brine, dried over Na_2SO_4, and concentrated to an oil that was purified by silica gel chromatography.

4-[*O*-Nitrofurfuryl *N*-Methyl-*N*-(4-chlorobutyl) Phosphono-(difluoromethyl)] Phenylacetic Acid (11). General procedure B with **10a** (0.040 g, 0.08 mmol), reaction time = 3 h. The product was purified by silica gel chromatography (20%EtOAc, 1% HCO_2H/hexane; 50% EtOAc, 1% HCO_2H/hexane; 70% EtOAc, 1% HCO_2H/hexane) and isolated as a pale yellow oil, 0.027 g (69%). $R_f = 0.48$, 70% EtOAc, 1% HCO_2H/hexane. ^1H NMR ($CDCl_3$): δ 7.52 (2H, d); 7.34 (2H, d); 7.20 (1H, d); 6.49 (1H, d); 5.02 (2H, dd); 3.68 (3H, s); 3.52 (2H, t); 3.05 (2H, m); 2.72 (3H, d); 1.70 (4H, m); ^{31}P NMR ($CDCl_3$): δ −10.78 (dd); HRMS ($C_{19}H_{22}ClF_2N_2O_7P$) calcd 517.0713 $(M + Na)^+$, found 517.0720.

Methyl 4-[*O*-Nitrofurfuryl *N*-Methyl-*N*-(4-chlorobutyl) Phosphono(difluoromethyl)]-*N*-Fmoc-(L)-phenylalanine (12a). Compound **10b** (1.60 g, 2.10 mmol, 1 equiv) in THF/H_2O (30 mL/6 mL) reacted with LiOH/H_2O (0.3 M, 14 mL) as described in General Procedure A to provide the crude product as a foam. Purification by silica gel chromatography (25% EtOAc/hexane; 50% EtOAc/hexane; then 50% EtOAc, 1% HCO_2H/hexane) provided the product as a foam, 1.30 g (83%). $R_f = 0.52$, 70% EtOAc, 1% HCO_2H/hexane. ^1H NMR ($CDCl_3$): δ) 7.78 (2H, d); 7.58−7.21 (11H, m); 6.49 (1H, dd); 5.52 (1H, m); 4.97 (2H, m); 4.66 (1H, m); 4.44−4.35 (2H, m); 4.18 (1H, t); 3.50 (2H, m); 3.19 (2H, m); 3.00 (2H, m); 2.68 (3H, d); 1.60 (4H, m); ^{31}P NMR ($CDCl_3$): δ −10.58 (t); HRMS ($C_{35}H_{35}ClF_2N_3O_9P$) calcd 790.1479 $(M + 2Na)^+$, found 790.1469.

4-[*O*-Nitrofurfuryl *N*-Methyl-*N*-(4-chlorobutyl) Phosphono-(difluoromethyl)]-*N*-Fmoc-(L)-phenylalanine Amide (12b). Compound **12a** (0.41 g, 0.55 mmol, 1 equiv) in THF (5.7 mL) was treated with *N*-hydroxysuccinimide (0.06 g, 0.55 mmol, 1 equiv) and was cooled to 0 °C. Diisopropylcarbodiimide (0.13 mL, 0.82 mmol, 1.5 equiv) was added by syringe. The reaction mixture was stirred at 0 °C for 1.5 h, and a 1 M solution of NH_4HCO_3 (2.7 mL, 2.7 mmol, 5 equiv) was added. The reaction mixture was stirred for 20 h as the temperature gradually came to ambience. Solvent was removed under reduced pressure, CH_2Cl_2 (10 mL) was added, and the mixture was washed successively with 10 mL portions of 1 M HCl, saturated $NaHCO_3$, and brine. The organic phase was dried over Na_2SO_4 and concentrated. Purification by silica gel chromatography (50% EtOAc/hexane; 75% EtOAc/hexane) provided the product as a yellow oil, 0.21 g (52%). $R_f = 0.26$, 100% EtOAc. ^1H NMR ($CDCl_3$) δ 7.72 (2H, δ)); 7.54−7.25 (10H, m); 7.18 (1H, d); 6.51 (1H, d); 6.25 (1H, bs); 5.93 (1H, bs); 5.74 (1H, m); 4.94 (2H, m); 4.47−4.35 (3H, m); 4.15 (1H, t); 3.50 (2H, t); 3.11−2.99 (4H, m); 2.66 (3H, d); 1.67−1.57 (4H, m); ^{31}P NMR

($CDCl_3$): δ −10.33 (dd); HRMS ($C_{35}H_{36}ClF_2N_4O_8P$) calcd 767.1820 $(M + Na)^+$, found 767.1821.

4-[*O*-Nitrofurfuryl *N*-Methyl-*N*-(4-chlorobutyl) Phosphono-(difluoromethyl)] Phenylacetyl-L-aspartic Acid *β*-*t*-Butyl Ester α-Methyl Ester (14a). Compound **13** (0.25 g, 0.59 mmol) was dissolved in CH_2Cl_2 (3 mL), and the solution was cooled to 0 °C. A 0.17 M solution of DBU in CH_2Cl_2 (3.8 mL, 0.65 mmol, 1.1 equiv) was added. While this mixture stirred, a solution of **11** (0.29 g, 0.59 mmol, 1.0 equiv) and PyBOP (0.31 g, 0.59 mmol, 1.0 equiv) in CH_2Cl_2 (3 mL) was prepared and cooled to 0 °C. TLC (2% MeOH, 1% AcOH/CH_2Cl_2) of the first reaction mixture after 20 min at 0 °C showed no starting material remaining. Deprotected **13** was transferred to the solution of **11**, and DIEA (0.22 mL, 1.26 mmol, 2.1 equiv) was added. The solution was stirred at 0 °C for 10 min and at room temperature for 50 min. TLC (75% EtOAc/hexane) showed no **11** remaining and the appearance of a new less polar spot. The reaction mixture was quenched with saturated NH_4Cl (10 mL). The phases were separated, and the aqueous phase was extracted with CH_2Cl_2 (2 × 10 mL). The combined organic phases were washed with brine, dried over Na_2SO_4, and concentrated to a dark, viscous oil. Purification by silica gel chromatography (50% EtOAc/hexane; 75% EtOAc/hexane) provided the product **14a** as yellow oil, 0.32 g (79%) R_f = 0.35, 75% EtOAc/hexane. ^{1}H NMR ($CDCl_3$): δ 7.55 (2H, d); 7.35 (2H, d); 7.24 (1H, d); 6.55 (1H, d); 6.46 (1H, d); 5.00 (2H, m); 4.77 (1H, m); 3.71 (3H, s); 3.63 (2H, s); 3.53 (2H, t); 3.07 (2H, m); 2.91 (1H, dd); 2.69 (4H, m); 1.71−1.57 (4H, m); 1.36 (9H, s); ^{31}P NMR ($CDCl_3$): δ −10.37 (dd); HRMS ($C_{28}H_{37}ClF_2N_3O_{10}P$) calcd 702.1771 $(M + Na)^+$, found 702.1764.

4-[*O*-Nitrofurfuryl *N*-Methyl-*N*-(4-chlorobutyl) Phosphono-(difluoromethyl)] Phenylacetyl-L-aspartic Acid *β*-*t*-Butyl Ester (14b). Compound **14a** (0.24 g, 0.35 mmol, 1 equiv) in THF/H_2O (4.6 mL/0.91 mL) was reacted with 0.3 M LiOH/H_2O (2.30 mL, 0.70 mmol, 2 equiv) according to General Procedure A. The crude product was isolated as a yellow oil. Purification by silica gel chromatography (75%EtOAc/hexane, 100% EtOAc) provided the product **14b** as a pale yellow oil, 0.22 g (94%). R_f = 0.19, 4% MeOH, 1% HCO_2H/CH_2Cl_2. ^{1}H NMR ($CDCl_3$): δ 7.47 (2H, d); 7.33 (2H, d); 7.21 (1H, d); 6.82 (1H, t); 6.54 (1H, d); 4.99 (2H, m); 4.74 (1H, m); 3.62 (2H, s); 3.50 (2H, t); 3.02 (2H, m); 2.88 (1H, dd); 2.69 (4H, m); 1.67−1.55 (4H, m); 1.34 (9H, s); ^{31}P NMR ($CDCl_3$): δ −10.57 (dd); HRMS ($C_{27}H_{35}ClF_2N_3O_{10}P$) calcd 710.1428 $(M + 2Na)^+$, found 710.1427.

4-[*O*-Nitrofurfuryl *N*-Methyl-*N*-(4-chlorobutyl) Phosphono-(difluoromethyl)]phenylacetyl-L-aspartyl-*β*-*t*-butyl Ester 4-[*O*-Nitrofurfuryl-*N*-methyl-*N*-(4-chlorobutyl) Phosphono(difluoromethyl)]-*N*-Fmoc-L-phenylalanine Amide (15). Compound **12b** (0.16 g, 0.21 mmol) was dissolved in CH_2Cl_2 (3 mL), and the solution was cooled to 0 °C. A 0.17 M solution of DBU in CH_2Cl_2 (1.73 mL, 0.29 mmol, 1.4 equiv) was added. While this mixture stirred, a solution of **14b** (0.18 g, 0.27 mmol, 1.3 equiv) and PyBOP (0.14 g, 0.27 mmol, 1.3 equiv) in CH_2Cl_2/THF (3 mL/1 mL) was prepared and cooled to 0 °C. TLC (2% MeOH, 1% AcOH/CH_2Cl_2) of the first reaction mixture after 30 min at 0 °C showed no Fmoc-protected starting material remaining. Deprotected **12b** was transferred to the solution of **14b**, and DIEA (0.10 mL, 0.56 mmol, 2.7 equiv) was added. The reaction mixture was stirred at 0 °C for 10 min and at room temperature for 30 min. The reaction was quenched with saturated NH_4Cl (10 mL). The phases were separated, and the aqueous phase was extracted with CH_2Cl_2 (3 × 10 mL). The combined organic phases were washed with brine, dried over Na_2SO_4, and concentrated to a dark oil. Purification by silica gel chromatography (2% MeOH, 1% AcOH/CH_2Cl_2) provided the product **15** as a pale yellow oil, 0.090 g (37%). R_f = 0.38, 2% MeOH, 1% HCO_2H/CH_2Cl_2. ^{1}H NMR (CD_3COCD_3): δ 7.62−7.37 (10H, m); 6.81 (2H, d); 5.16 (4H, m); 4.77 (2H, m); 3.67 (2H, s); 3.58 (4H, t); 3.06−2.95 (6H, m); 2.75 (2H, m); 2.68 (6H, d); 1.72−1.55 (8H, m); 1.38 (9H, s); ^{31}P NMR (acetone-d_6): δ −9.90 (t).

4-[*O*-Nitrofurfuryl *N*-Methyl-*N*-(4-chlorobutyl) Phosphono-(difluoromethyl)]phenylacetyl-(L)-aspartyl-4-[*O*-nitrofurfuryl *N*-Methyl-*N*-(4-chlorobutyl) Phosphono(difluoromethyl)]-*N*-Fmoc-(L)-phenylalanine Amide (1b). Compound **15** (0.067 g, 0.058 mmol) in CH_2Cl_2 (1.1 mL) was treated with TFA (0.57 mL), and the reaction mixture was stirred at room temperature for 1.5 h. The reaction was quenched with 5 mL of H_2O and extracted with EtOAc (4 × 10 mL). The combined organic extracts were washed successively with 5 mL portions of water and brine, then were dried over Na_2SO_4 and concentrated to a yellow oil. Purification by silica gel chromatography (100% EtOAc; 2% MeOH, 1% AcOH/CH_2Cl_2; 4% MeOH, 1% AcOH/CH_2Cl_2) provided the product **1b** as a pale yellow oil, 0.049 g (77%). R_f = 0.21, 4% MeOH, 1% HCO_2H/CH_2Cl_2. ^{1}H NMR (CD_3OD): δ 8.10 (4H, bs); 7.47−7.35 (10H, m); 6.75 (2H, m); 5.09 (4H, m); 4.65 (1H, t); 4.57 (1H, m); 3.61−3.54 (6H, m); 3.10−2.95 (6H, m); 2.68 (6H, d); 2.63 (2H, m); 1.68−1.60 (8H, m); ^{31}P NMR (CD_3OD): δ −9.85 (t); ^{13}C NMR (CD_3OD): δ 173.67 (s); 173.32 (s); 173.04 (s); 172.82 (s); 172.66 (s); 153.79 (s); 153.32 (s); 142.03 (s); 139.94 (s); 132.45 (s); 130.60 (d); 127.34 (d); 115.19 (d); 113.23 (d); 59.92 (t); 55.44 (d); 51.72 (d); 51.41 (d); 49.32 (t); 45.39 (t); 43.02 (t); 38.28 (t); 36.61 (t); 33.78 (q); 30.55 (t); 26.10 (t); HPLC: flow rate = 1 mL/min, retention time = 14.5 min, C18 column, 50% CH_3CN/H_2O; 5.4 min, phenyl column, 30% CH_3CN/H_2O.

Acknowledgment. We appreciate the helpful discussions with Christine O'Day throughout the course of this project. Financial Support from the NCI (R01 CA34619 to R.F.B.) and NIDDK (RO1 DK68447 to Z.-Y.Z.) is gratefully acknowledged. Support from the Purdue Cancer Center Support Grant P30 CA23168 for services provided by the NMR and Mass Spectrometry Shared Resources is appreciated.

References

(1) Hunter, T. Signaling−2000 and beyond. *Cell* **2000**, *100*, 113−27.
(2) Zhang, Z. Y. Protein tyrosine phosphatases: prospects for therapeutics. *Curr. Opin. Chem. Biol.* **2001**, *5*, 416−23.
(3) Lund, I. K.; Andersen, H. S.; Iversen, L. F.; Olsen, O. H.; Moller, K. B.; Pedersen, A. K.; Ge, Y.; Holsworth, D. D.; Newman, M. J.; Axe, F. U.; Moller, N. P. Structure-based design of selective and potent inhibitors of protein-tyrosine phosphatase beta. *J. Biol. Chem.* **2004**, *279*, 24226−35.
(4) Blume-Jensen, P.; Hunter, T. Oncogenic kinase signalling. *Nature* **2001**, *411*, 355−65.
(5) Ventura, J. J.; Nebreda, A. R. Protein kinases and phosphatases as therapeutic targets in cancer. *Clin. Trans. Oncol.* **2006**, *8*, 153−60.
(6) Goldman, J. M.; Melo, J. V. Targeting the BCR-ABL tyrosine kinase in chronic myeloid leukemia. *N. Engl. J. Med.* **2001**, *344*, 1084−6.
(7) Berman, J.; O'Leary, T. J. Gastrointestinal stromal tumor workshop. *Hum. Pathol.* **2001**, *32*, 578−82.
(8) Li, L.; Dixon, J. E. Form function and regulation of protein tyrosine phosphatases and their involvement in human diseases. *Semin. Immunol.* **2000**, *12*, 75−84.
(9) Bourdeau, A.; Dube, N.; Tremblay, M. L. Cytoplasmic protein tyrosine phosphatases regulation and function: the roles of PTP1B and TC-PTP. *Curr. Opin. Cell Biol.* **2005**, *17*, 203−9.
(10) Zhang, Z. Protein tyrosine phosphatases: structure and function, substrate specificity, and inhibitor development. *Ann. Rev. Pharmacol. Toxicol.* **2002**, *42*, 209−34.
(11) Burke, T. R., Jr; Zhang, Z.-Y. Protein−tyrosine phosphatases: structure mechanism and inhibitor discovery. *Biopolymers* **1998**, *47*, 225−41.
(12) Zhang, Z.-Y. Inhibitors of protein tyrosine phosphatases. In *Handbook of Cell Signaling*, 1st ed.; Bradshaw, R., Dennis, E., Eds; Academic Press: New York, 2003; pp 677−684.
(13) Burke, T. R., Jr; Kole, H. K.; Roller, P. P. Potent inhibition of insulin receptor dephosphorylation by a hexamer peptide containing the phosphotyrosyl mimetic F2Pmp. *Biochem. Biophys. Res. Commun.* **1994**, *204*, 129−34.
(14) Chen, L.; Wu, L.; Otaka, A.; Smyth, M. S.; Roller, P. P.; Burke, T. R., Jr; den Hertog, J.; Zhang, Z.-Y. Why is phosphonodifluoromethyl phenylalanine a more potent inhibitory moiety than phosphonomethyl phenylalanine toward protein−tyrosine phosphatases? *Biochem. Biophys. Res. Commun.* **1995**, *216*, 976−84.
(15) Shen, K.; Keng, Y. F.; Wu, L.; Guo, X. L.; Lawrence, D. S.; Zhang, Z.-Y. Acquisition of a specific and potent PTP1B inhibitor from a novel combinatorial library and screening procedure. *J. Biol. Chem.* **2001**, *276*, 47311−9.

(16) Dufresne, C.; Roy, P.; Wang, Z.; Asante-Appiah, E.; Cromlish, W.; Boie, Y.; Forghani, F.; Desmarais, S.; Wang, Q.; Skorey, K.; Waddleton, D.; Ramachandran, C.; Kennedy, B. P.; Xu, L.; Gordon, R.; Chan, C. C.; Leblanc, Y. The development of potent non-peptidic PTP 1B inhibitors. *Bioorg. Med. Chem. Lett.* **2004**, *14*, 1039−42.
(17) Lau, C. K.; Bayly, C. I.; Gauthier, J. Y.; Li, C. S.; Therien, M.; Asante-Appiah, E.; Cromlish, W.; Boie, Y.; Forghani, F.; Desmarais, S.; Wang, Q.; Skorey, K.; Waddleton, D.; Payette, P.; Ramachandran, C.; Kennedy, B. P.; Scapin, G. Structure-based design of a series of potent and selective non-peptidic PTP 1B inhibitors. *Bioorg. Med. Chem. Lett.* **2004**, *14*, 1043−8.
(18) Elchebly, M.; Payette, P.; Michaliszyn, E.; Cromlish, W.; Collins, S.; Loy, A. L.; Normandin, D.; Cheng, A.; Himms-Hagen, J.; Chan, C. C.; Ramachandran, C.; Gresser, M. J.; Tremblay, M. L.; Kennedy, B. P. Increased insulin sensitivity and obesity resistance in mice lacking the protein tyrosine phosphatase 1B gene. *Science* **1999**, *283*, 1544−8.
(19) Klaman, L. D.; Boss, O.; Peroni, O. D.; Kim, J. K.; Martino, J. L.; Zabolotny, J. M.; Moghal, N.; Lubkin, M.; Kim, Y. B.; Sharpe, A. H.; Stricker-Krongrad, A.; Shulman, G. I.; Neel, B. G.; Kahn, B. B. Increased energy expenditure decreased adiposity and tissue-specific insulin sensitivity in protein-−tyrosine phosphatase 1B deficient mice. *Mol. Cell Biol.* **2000**, *20*, 5479−89.
(20) Zhang, Z.-Y.; Lee, S. Y. PTP1B inhibitors as potential therapeutics in the treatment of type 2 diabetes and obesity. *Expert Opin. Investig. Drugs* **2003**, *12*, 223−33.
(21) Xie, L.; Lee, S. Y.; Andersen, J. N.; Waters, S.; Shen, K.; Guo, X. L.; Moller, N. P.; Olefsky, J. M.; Lawrence, D. S.; Zhang, Z.-Y. Cellular effects of small molecule PTP1B inhibitors on insulin signaling. *Biochemistry* **2003**, *42*, 12792−804.
(22) Lee, S. Y.; Liang, F.; Guo, X. L.; Xie, L.; Cahill, S. M.; Blumenstein, M.; Yang, H.; Lawrence, D. S.; Zhang, Z.-Y. Design, construction, and intracellular activation of an intramolecularly self-silenced signal transduction inhibitor. *Angew. Chem., Int. Ed.* **2005**, *44*, 4242−4.
(23) Liang, F.; Lee, S. Y.; Liang, J.; Lawrence, D. S.; Zhang, Z.-Y. The role of protein−tyrosine phosphatase 1B in integrin signaling. *J. Biol. Chem.* **2005**, *280*, 24857−63.
(24) Lee, H.; Xie, L.; Luo, Y.; Lee, S. Y.; Lawrence, D. S.; Wang, X. B.; Sotgia, F.; Lisanti, M. P.; Zhang, Z.-Y. Identification of phosphocaveolin-1 as a novel protein−tyrosine phosphatase 1B substrate. *Biochemistry* **2006**, *45*, 234−40.
(25) Dang, Q. Organophosphonic acids as drug candidates. *Expert Opin. Ther. Patents* **2006**, *16*, 343−8.
(26) Stankovic, C. J.; Surendran, N.; Lunney, E. A.; Plummer, M. S.; Para, K. S.; Shahripour, A.; Fergus, J. H.; Marks, J. S.; Herrera, R.; Hubbell, S. E.; Humblet, C.; Saltiel, A. R.; Stewart, B. H.; Sawyer, T. K. The role of 4-phosphonodifluoromethyl- and 4-phosphonophenylalanine in the selectivity and cellular uptake of SH2 domain ligands. *Bioorg. Med. Chem. Lett.* **1997**, *7*, 1904−9.
(27) Freel Meyers, C. L.; Hong, L.; Joswig, C.; Borch, R. F. Synthesis and biological activity of novel 5-fluoro-2′-deoxyuridine phosphoramidate prodrugs. *J. Med. Chem.* **2000**, *43*, 4313−8.
(28) Tobias, S. C.; Borch, R. F. Synthesis and biological studies of novel nucleoside phosphoramidate prodrugs. *J. Med. Chem.* **2001**, *44*, 4475−80.
(29) Garrido-Hernandez, H.; Moon, K. D.; Geahlen, R. L.; Borch, R. F. Design and synthesis of phosphotyrosine peptidomimetic prodrugs. *J. Med. Chem.* **2006**, *49*, 3368−76.
(30) Terauchi, K.; Sakurai, H. Photochemical studies of esters of aroylphosphonic acids. *Bull. Chem. Soc. Jpn.* **1970**, *43*, 883−90.
(31) Burke, T. R.; Smyth, M. S.; Otaka, A.; Roller, P. P. Synthesis of 4-phosphono(difluoromethyl)-D,L-phenylalanine and *N*-boc and *N*-fmoc derivatives suitably protected for solid phase synthesis of nonhydrolyzable phosphotyrosyl peptide analogues. *Tetrahedron Lett.* **1993**, *34*, 4125−8.
(32) Qabar, M. N.; Urban, J.; Kahn, M. A facile solution and solid phase synthesis of phosphotyrosine mimetic L-4-[diethylphosphono(difluoromethyl)]-phenylalanine (F2Pmp(EtO)$_2$ derivatives. *Tetrahedron* **1997**, *53*, 11171−8.
(33) Yang, G.; Chun, J.; Arakawa-Uramoto, H.; Wang, X.; Gawinowicz, M. A.; Zhao, K.; Landry, D. W. Anti-cocaine catalytic antibodies: a synthetic approach to improved antibody diversity. *J. Am. Chem. Soc.* **1996**, *118*, 5881−90.
(34) Namikoshi, M.; Kundu, B.; Rinehart, K. L. Use of tetrabutylammonium fluoride as a facile deprotecting reagent for 4-nitrobenzyl, 2,2,2-trichloroethyl, and phenacyl esters of amino acids. *J. Org. Chem.* **1991**, *56*, 5464−6.
(35) Nicolaou, K. C.; Estrada, A. A.; Zak, M.; Lee, S. H.; Safina, B. S. A mild and selective method for the hydrolysis of esters with trimethyltin hydroxide. *Angew. Chem., Int. Ed.* **2005**, *44*, 1378−82.
(36) Guo, X. L.; Shen, K.; Wang, F.; Lawrence, D. S.; Zhang, Z.-Y. Probing the molecular basis for potent and selective protein−tyrosine phosphatase 1B inhibition. *J. Biol. Chem.* **2002**, *277*, 41014−22.
(37) Sun, J. P.; Fedorov, A. A.; Lee, S. Y.; Guo, X. L.; Shen, K.; Lawrence, D. S.; Almo, S. C.; Zhang, Z.-Y. Crystal structure of PTP1B complexed with a potent and selective bidentate inhibitor. *J. Biol. Chem.* **2003**, *278*, 12406−14.
(38) White, M. F. The IRS-signaling system: a network of docking proteins that mediate insulin action. *Mol. Cell Biochem.* **1998**, *182*, 3−11.
(39) Saltiel, A. R.; Kahn, C. R. Insulin signaling and the regulation of glucose and lipid metabolism. *Nature* **2001**, *414*, 799−806.
(40) Clampit, J. E.; Meuth, J. L.; Smith, H. T.; Reilly, R. M.; Jirousek, M. R.; Trevillyan, J. M.; Rondinone, C. M. Reduction of protein−tyrosine phosphatase 1B increases insulin signaling in FAO hepatoma cells. *Biochem. Biophys. Res. Commun.* **2003**, *300*, 261−7.

JM061146X